Punjab University Journal of Mathematics (2025), 57(08), 896- 914
https://doi.org/10.52280/pujm.2025.57(08)05

Insights into Engineering Shapes through Curve and Surface Modeling with the 4-Point Quaternary Subdivision Scheme

Received
02 September, 2025

Revised
05 December, 2025

Accepted
16 December, 2025

Published Online
23 December, 2025

Muhammad Tahseen Iqbal
Department of Mathematics, The Islamia University of Bahawalpur, Pakistan

Rakib Mustafa
Department of Computer Systems Engineering, The Islamia University of Bahawalpur, Pakistan

Ghulam Mustafa
Department of Mathematics, The Islamia University of Bahawalpur, Pakistan

Humaira Mustanira Tariq
Department of Mathematics, The Islamia University of Bahawalpur, Pakistan

Samsul Ariffin Abdul Karim
Institute of Strategic Industrial Decision Modelling (ISIDM), School of Quantitative Sciences, UUM College of Arts & Sciences, Universiti Utara Malaysia, 06010 Sintok, Kedah Darul Aman, Malaysia
Computational Statistics and Applied Mathematics (CSAM) Research Group, School of Quantitative Sciences, UUM College of Arts & Sciences, Universiti Utara Malaysia, 06010 Sintok, Kedah Darul Aman, Malaysia

Abstract. Curve and surface modeling is an essential area of computer graphics that involves the creation of complex geometries and shapes used in various industries and engineering disciplines, such as automotive, architecture, and entertainment. Subdivision schemes are among the best-known and most widely applied methods for generating smooth shapes. Convexity and monotonicity are important geometric properties in shape design for engineering applications, as they help ensure that shapes are structurally sound, manufacturable, and exhibit desirable performance characteristics. While the smoothness of a shape is measured in terms of the order of continuity, preserving geometric properties such as convexity and monotonicity remains a challenging task. Keeping this in view, a 4-point quaternary subdivision scheme is proposed, and its geometric properties are analyzed for a certain range of parameters. Several examples, including real-life and engineering-based graphical objects, are presented on curves and surfaces to demonstrate the smoothness and shape-preserving capability of the proposed scheme.

Corresponding Author: ghulam.mustafa@iub.edu.pk

AMS (MOS) Subject Classification Codes: 65D17, 65D07, 65D05.
Key Words: Shape design; smoothness; convexity; monotonicity; engineering; subdivision curve and surface; shape parameters

1. Introduction

Computer Aided Graphic Designs (CAGD) is a computational mathematics research field that focuses on geometric objects used to approximate discrete or scattered data with curves or surfaces. Naval architecture, aeronautics, and the automobile industry initially made extensive use of this field. CAGD emerged as a distinct discipline following a conference at the University of Utah [11].

Subdivision schemes generally refine data and increase the number of data points through successive iterations. These schemes are computationally efficient because they can generate curves and surfaces in a recursive and stable manner. Subdivision schemes can generally be classified into two categories: interpolatory and approximating subdivision schemes. Interpolatory subdivision schemes produce a limiting curve that passes through all the input data points, while approximating subdivision schemes do not necessarily interpolate the initial data set.

Subdivision schemes play a fundamental role in computer-aided geometric design and signal processing. Theoretical foundations on convergence and regularity were established by Dyn and Rioul [5, 19], while comprehensive treatments in geometric modelling were presented by Dyn and Levin [6]. Convexity-preserving subdivision schemes were studied by Le Méhauté and Utreras [12], and important advances in approximation order and nonlinear subdivision methods were reported in [4, 2].

Both categories of schemes are designed to efficiently preserve shape properties such as monotonicity and convexity of the initial control polygon [11]. In [7], conditions on the scheme parameters are applied to maintain convexity in the four-point binary scheme. A convexity-preserving algorithm for the four-point binary scheme is presented in [3]. A shape-preserving scheme was also presented in [23]. Akram et al. [1] presented the convexity and monotonicity preservation of a ternary 4-point approximating scheme. Iqbal et al. [9] studied the convexity preservation of a 6-point ternary interpolating scheme. Combined interpolatory and approximating 4-point ternary schemes were developed and discussed in [24].

Quaternary subdivision schemes are more advanced than lower-arity (i.e., binary and ternary) schemes. These schemes allow greater control over curve fitting and exhibit faster convergence towards the final limit curve [18]. Increasing the arity of a subdivision scheme generally results in higher smoothness of the limit function. A 4-point quaternary subdivision scheme with a single shape parameter was developed in [16]. A 3-point relaxed nonsymmetric approximating stationary quaternary subdivision scheme with two parameters was discussed in [22]. In [14], a generalized formulation for the construction of multi-parameter quaternary schemes was presented. A 7-point quaternary subdivision scheme with a shape parameter was introduced in [17], and its properties were analyzed for different parameter values.

Ko [10] presented a 4-point quaternary scheme, while Siddiqi and Younis [21] proposed an m-point quaternary scheme. The subdivision depth of quaternary schemes was investigated in [20]. A comprehensive review of subdivision schemes is presented by Liu et al. [13].

In this study, we investigate the efficiency of a 4-point quaternary subdivision scheme in curve and surface modeling. We demonstrate that the scheme exhibits versatility in generating a wide variety of visual shapes suitable for engineering and industrial applications. The scheme is applied to fit discrete data and generate representative shapes, including English alphabets and common engineering tools such as hammers, pickaxes, spanners, fan blades, fighter planes, and fighter jets. The proposed quaternary scheme is shown to be capable of producing convex and monotone shapes within specific ranges of the scheme parameters.

The remainder of the paper is organized as follows. Section 1 presents the introduction and provides the research motivation and objectives. Section 2 details the construction of the proposed subdivision scheme. Section 3 analyzes the scheme and discusses its continuity properties, along with a comparison with existing 4-point quaternary schemes. Section 4 is devoted to the convexity and monotonicity analysis. Section 5 presents the quantitative error analysis, computational complexity, and convergence benchmark of the proposed scheme, along with a comparison with existing schemes. Section 6 demonstrates practical applications of the proposed scheme using real-world data. Finally, Section 7 concludes the paper and highlights directions for future research.

2. The construction of a 4-point quaternary scheme

A general form of quaternary subdivision scheme $S_{\varepsilon_{\alpha,\beta}}$ that maps $f^k = \{f_i^k, i \in \mathbb{Z}\}$ to a refined polygon $f^{k+1} = \{f_i^{k+1}, i \in \mathbb{Z}\}$ is defined as

$$f_i^{k+1} = \sum_{j \in \mathbb{Z}} (\varepsilon_{\alpha,\beta})_{i-4j} f_i^k, \ i \in \mathbb{Z}.$$

A polynomial, generated by the coefficients $\varepsilon_{\alpha,\beta}$ of a subdivision scheme, called the Laurent polynomial of the subdivision scheme $S_{\varepsilon_{\alpha,\beta}}$, is defined as

$$\varepsilon_{\alpha,\beta}(z) = \sum_{i \in \mathbb{Z}} (\varepsilon_{\alpha,\beta})_i z^i, \ \text{where } (\varepsilon_{\alpha,\beta})_i \text{ is also called the mask of the scheme.}$$

The necessary condition for the convergence of the quaternary subdivision scheme is

$$\sum_{i \in \mathbb{Z}} (\varepsilon_{\alpha,\beta})_{4i} = \sum_{i \in \mathbb{Z}} (\varepsilon_{\alpha,\beta})_{4i+1} = \sum_{i \in \mathbb{Z}} (\varepsilon_{\alpha,\beta})_{4i+2} = \sum_{i \in \mathbb{Z}} (\varepsilon_{\alpha,\beta})_{4i+3} = 1.$$

It follows that the Laurent polynomial of the convergent subdivision scheme satisfies the condition. $\varepsilon_{\alpha,\beta}(e^{\frac{ni\pi}{4}}) = 0$ and $\varepsilon_{\alpha,\beta}(1) = 4$ for $n = 1, 2, 3, 4$.

Subdivision schemes vary in their coefficients and in the number of points used to generate new points. They also differ in the rules employed to determine these points. For instance, a quaternary subdivision scheme utilizes four distinct refinement rules. In this work, we propose the construction of a new 4-point quaternary subdivision scheme. To construct this scheme, we combine two existing schemes: an interpolatory subdivision scheme [15], defined in (2. 1), and an approximating subdivision scheme [16], defined in (2. 2). First, we compute the difference mask between these two schemes, as given in (2. 3). Then, we perform a linear combination of the schemes in (2. 3) and (2. 1). This process yields the proposed subdivision scheme, which is formally defined in (2. 4).
The 4-point quaternary interpolating subdivision scheme [15] can be expressed as follows:

$$\begin{cases} L_{4\,i}^{k+1} &= f_i^k \\ L_{4i+1}^{k+1} &= -\frac{7}{128} f_{i-1}^k + \frac{105}{128} f_i^k + \frac{35}{128} f_{i+1}^k - \frac{5}{128} f_{i+2}^k \\ L_{4\,i+2}^{k+1} &= -\frac{1}{16} f_{i-1}^k + \frac{9}{16} f_i^k + \frac{9}{16} f_{i+1}^k - \frac{1}{16} f_{i+2}^k \\ L_{4\,i+3}^{k+1} &= -\frac{5}{128} f_{i-1}^k + \frac{35}{128} f_i^k + \frac{105}{128} f_{i+1}^k - \frac{7}{128} f_{i+2}^k \end{cases} \tag{2. 1}$$

here, L_i^{k+1} represents the refined points. The refinement rules of the 4-point approximating scheme [16] with parameter $\omega = 0$ can be written as

$$\begin{cases} Q_{4\,i}^{k+1} &= \frac{7}{32} f_{i-1}^k + \frac{29}{64} f_i^k + \frac{5}{16} f_{i+1}^k + \frac{1}{64} f_{i+2}^k \\ Q_{4\,i+1}^{k+1} &= \frac{15}{128} f_{i-1}^k + \frac{57}{128} f_i^k + \frac{49}{128} f_{i+1}^k + \frac{7}{128} f_{i+2}^k \\ Q_{4\,i+2}^{k+1} &= \frac{7}{128} f_{i-1}^k + \frac{49}{128} f_i^k + \frac{57}{128} f_{i+1}^k + \frac{15}{128} f_{i+2}^k \\ Q_{4\,i+3}^{k+1} &= \frac{1}{64} f_{i-1}^k + \frac{5}{16} f_i^k + \frac{29}{64} f_{i+1}^k + \frac{7}{32} f_{i+2}^k \end{cases} \tag{2. 2}$$

where, Q_i^{k+1} represents the refined points. The displacement vectors are obtained by using the following relation: $D_{4\,i}^{k+1} = Q_{4\,i}^{k+1} - L_{4\,i}^{k+1}$, $D_{4\,i+1}^{k+1} = Q_{4\,i+1}^{k+1} - L_{4\,i+1}^{k+1}$, $D_{4\,i+2}^{k+1} = Q_{4\,i+2}^{k+1} - L_{4\,i+2}^{k+1}$ and $D_{4\,i+3}^{k+1} = Q_{4\,i+3}^{k+1} - L_{4\,i+3}^{k+1}$. Which can be written as

$$\begin{pmatrix} D_{4i}^{k+1} \\ D_{4i+1}^{k+1} \\ D_{4i+2}^{k+1} \\ D_{4i+3}^{k+1} \end{pmatrix} = \frac{1}{128} \begin{pmatrix} 28 & -70 & 40 & 2 \\ 22 & -48 & 14 & 12 \\ 15 & -23 & -15 & 23 \\ 7 & 5 & -47 & 35 \end{pmatrix} \begin{pmatrix} f_{i-1}^k \\ f_i^k \\ f_{i+1}^k \\ f_{i+2}^k \end{pmatrix}. \tag{2. 3}$$

A combined quaternary subdivision scheme with two parameters can be obtained by translating the points $L_{4\,i}^{k+1}$, $L_{4\,i+1}^{k+1}$, $L_{4\,i+2}^{k+1}$ and $L_{4\,i+3}^{k+1}$ of (2. 1) to a new position.

$$\begin{pmatrix} f_{4i}^{k+1} \\ f_{4i+1}^{k+1} \\ f_{4i+2}^{k+1} \\ f_{4i+3}^{k+1} \end{pmatrix} = \begin{pmatrix} L_{4i}^{k+1} \\ L_{4i+1}^{k+1} \\ L_{4i+2}^{k+1} \\ L_{4i+3}^{k+1} \end{pmatrix} + \begin{pmatrix} \alpha-\beta & 0 & 0 & 0 \\ 0 & \alpha-\beta & 0 & 0 \\ 0 & 0 & \alpha-\beta & 0 \\ 0 & 0 & 0 & \alpha-\beta \end{pmatrix} \begin{pmatrix} D_{4i}^{k+1} \\ D_{4i+1}^{k+1} \\ D_{4i+2}^{k+1} \\ D_{4i+3}^{k+1} \end{pmatrix}.$$

The refinement rules for the proposed quaternary subdivision scheme are

$$\begin{pmatrix} f_{4i}^{k+1} \\ f_{4i+1}^{k+1} \\ f_{4i+2}^{k+1} \\ f_{4i+3}^{k+1} \end{pmatrix} = \frac{\Delta}{128} \begin{pmatrix} f_{i-1}^{k} \\ f_{i}^{k} \\ f_{i+1}^{k} \\ f_{i+2}^{k} \end{pmatrix} \tag{2. 4}$$

where

$$\Delta = \begin{pmatrix} -28\beta+28\alpha & 128-70\alpha+70\beta & -40\beta+40\alpha & -2\beta+2\alpha \\ -7-22\beta+22\alpha & 105+48\beta-48\alpha & 35-14\beta+14\alpha & -5-12\beta+12\alpha \\ -8-15\beta+15\alpha & 72+23\beta-23\alpha & 72+15\beta-15\alpha & -8-23\beta+23\alpha \\ -5-7\beta+7\alpha & 35-5\beta+5\alpha & 105+47\beta-47\alpha & -7-35\beta+35\alpha \end{pmatrix}$$

$$\begin{matrix} -2\beta+2\alpha \\ -5-12\beta+12\alpha \\ -8-23\beta+23\alpha \\ -7-35\beta+35\alpha \end{matrix} \Bigg).$$

3. Mathematical analysis of the scheme

In this section, we provide a rigorous mathematical analysis of the anticipated smoothness of the engineering shapes produced by the proposed scheme. To this end, we determine the order of continuity exhibited by the scheme for various values of the scheme parameters. Additionally, we present predictions of higher-order smoothness by computing the Hölder regularity of the scheme. Moreover, we demonstrate the polynomial reproduction and polynomial generation capabilities of the proposed scheme in this section.

Subdivision schemes are inherently discrete in nature. To analyze their properties effectively, the mask representation alone may not provide sufficient analytical insight. As a remedy, a polynomial representation known as the Laurent polynomial is introduced. Specifically, for the proposed subdivision scheme (2. 4), the corresponding Laurent polynomial is defined as follows:

$$\begin{aligned} \varepsilon_{\alpha,\beta}(z) \quad = \quad & \frac{1}{128}\Big[(-5+7\alpha-7\beta)+(-8+15\alpha-15\beta)\,z+(-7+22\alpha-22\beta)\,z^2 \\ & +(28\alpha-28\beta)\,z^3+(35+5\alpha-5\beta)\,z^4+(72-23\alpha+23\beta)\,z^5+(105 \\ & -48\alpha+48\beta)z^6+(128-70\alpha+70\beta)\,z^7+(105-47\alpha+47\beta)\,z^8 \\ & +(72-15\alpha+15\beta)\,z^9+(35+14\alpha-14\beta)\,z^{10}+(40\alpha-40\beta)\,z^{11} \\ & +(-7+35\alpha-35\beta)\,z^{12}+(-8+23\alpha-23\beta)\,z^{13}+(-5+12\alpha-12\beta)\,z^{14} \\ & +(-2\beta+2\alpha)\,z^{15}\Big]. \end{aligned} \tag{3. 5}$$

It can be rewritten as

$$\begin{aligned}\varepsilon_{\alpha,\beta}(z) &= \frac{1}{128}(z^3+z^2+z+1)^4\Big[(-5-7\beta+7\alpha)z^0+(12-13\alpha+13\beta)z \\ &\quad +(-5+4\alpha-4\beta)z^2+(-2\beta+2\alpha)z^3\Big] \qquad (3.\ 6)\end{aligned}$$

or as

$$\begin{aligned}\varepsilon_{\alpha,\beta}(z) &= \left(\frac{z^3+z^2+z+1}{4}\right)^4\Big[(-10-14\beta+14\alpha)z^0+(24-26\alpha+26\beta)z \\ &\quad +(-10+8\alpha-8\beta)z^2+(-4\beta+4\alpha)z^3\Big]. \qquad (3.\ 7)\end{aligned}$$

3.1. **Continuity analysis.** In mathematics, the smoothness of a curve or surface is measured in terms of continuity; the higher the continuity, the greater the smoothness. The closest intuitive meaning of continuity is controllability, which implies that one can ensure an acceptably close output by controlling the input within a sufficiently small neighborhood of the desired value. The practical significance of continuity lies in the fact that it helps us understand which mathematical functions can be physically realized in the real world. In this section, we identify the admissible parameter ranges required to produce output shapes with different levels of smoothness, commonly referred to as the order of continuity.

Theorem 3.2. *A proposed 4-point quaternary subdivision scheme defined by (2. 4) is C^0-continuous for the parametric interval $-\frac{23}{10}<\alpha<\frac{41}{10}$, $\beta=0$ and $-\frac{41}{10}<\beta<\frac{23}{10}$, $\alpha=0$.*

Proof. For the C^0-continuity of the subdivision scheme (2. 4) corresponding to the Laurent polynomial $\varepsilon_{\alpha,\beta}(z)$, it is sufficient to show that the subdivision scheme associated with the Laurent polynomial $b_0(z)$ is convergent. To this end, we construct the corresponding difference scheme derived from the polynomial $b_0(z)$, whose associated Laurent polynomial is denoted by $c_0(z)$. From (3. 6),

$$\varepsilon_{\alpha,\beta}(z)=\left(\frac{z^3+z^2+z+1}{4}\right)^0 b_0(z)$$

where

$$\begin{aligned}b_0(z) &= \frac{1}{128}(z^3+z^2+z+1)^4\Big[(-5-7\beta+7\alpha)z^0+(12-13\alpha+13\beta)z \\ &\quad +(-5+4\alpha-4\beta)z^2+(-2\beta+2\alpha)z^3\Big].\end{aligned}$$

Or, $b_0(z)=(z^3+z^2+z+1)c_0(z)$, where

$$\begin{aligned}c_0(z) &= \frac{1}{128}\left(z^3+z^2+z+1\right)^3\Big[\left(-2\beta+2\alpha\right)z^3+\left(-4\beta+4\alpha-5\right)z^2+(13\beta \\ &\quad -13\alpha+12)z+(-7\beta+7\alpha-5)\Big].\end{aligned}$$

If the subdivision scheme corresponding to $c_0(z)$ is contractive, then the subdivision scheme associated with $b_0(z)$ is convergent. Consequently, the subdivision scheme (2. 4) is C^0-continuous.

$$\begin{aligned} c_0(z) \;=\; & \frac{1}{128}\Big[(-2\beta+2\alpha)z^{12}+(10\alpha-10\beta-5)\,z^{11}+(11\alpha-11\beta-3)\,z^{10} \\ & +(12\alpha-12\beta+1)\,z^{9}+(7\alpha-7\beta+7)\,z^{8}+(-16\alpha+16\beta+30)\,z^{7} \\ & +(-18\alpha+18\beta+34)\,z^{6}+(-20\alpha+20\beta+34)\,z^{5}+(-16\alpha+16\beta \\ & +30)z^{4}+(6\alpha-6\beta+7)\,z^{3}+(7\alpha-7\beta+1)\,z^{2}+(8\alpha-8\beta-3)\,z \\ & +(7\alpha-7\beta-5)\Big]. \end{aligned} \tag{3. 8}$$

This implies that

$$c_0(z)=\sum_{i=0}^{12} r_0^i z^i$$

where
$r_0^0=7\alpha-7\beta-5,\quad r_0^1=8\alpha-8\beta-3,\quad r_0^2=7\alpha-7\beta+1,\quad r_0^3=6\alpha-6\beta+7,$
$r_0^4=-16\alpha+16\beta+30,\quad r_0^5=-20\alpha+20\beta+34,\quad r_0^6=-18\alpha+18\beta+34,$
$r_0^7=-16\alpha+16\beta+30,\quad r_0^8=7\alpha-7\beta+7,\quad r_0^9=12\alpha-12\beta+1,\quad r_0^{10}=11\alpha-11\beta-3,$
$r_0^{11}=10\alpha-10\beta-5,\quad r_0^{12}=-2\beta+2\alpha.$
Therefore

$$\begin{aligned} \sum_{i=0}^{3}|r_0^{4i}| &= \frac{1}{128}\Big[2|-\beta+\alpha|+7|\alpha-\beta+1|+2|8\alpha-8\beta-15|+|7\alpha-7\beta-5|\Big] \\ \sum_{i=0}^{2}|r_0^{4i+1}| &= \frac{1}{128}\Big[|12\alpha-12\beta+1|+2|10\alpha-10\beta-17|+|8\alpha-8\beta-3|\Big] \\ \sum_{i=0}^{2}|r_0^{4i+2}| &= \frac{1}{128}\Big[|11\alpha-11\beta-3|+2|9\alpha-9\beta-17|+|7\alpha-7\beta+1|\Big] \\ \sum_{i=0}^{2}|r_0^{4i+3}| &= \frac{1}{128}\Big[5|2\alpha-2\beta-1|+2|8\alpha-8\beta-15|+|6\alpha-6\beta+7|\Big] \end{aligned}$$

where r_0^i are the coefficients of z in (3. 8). We verify the contractiveness of the subdivision scheme S_{c_0} corresponding to $c_0(z)$ by computing its infinity norm as follows:

$$||S_{c_0}||_\infty \;=\; \max\Big[\sum_{i=0}^{3}|r_0^{4i}|,\, \sum_{i=0}^{2}|r_0^{4i+1}|,\, \sum_{i=0}^{2}|r_0^{4i+2}|,\, \sum_{i=0}^{2}|r_0^{4i+3}|\Big].$$

Scheme	Nature	Continuity
4-point quaternary [18]	Approximating	C^1
4-point quaternary [22]	Approximating	C^3
4-point quaternary [14]	Approximating	C^3
4-point quaternary[10]	Approximating	C^2
4-point quaternary [10]	Interpolating	C^2
4-point quaternary [21]	Approximating	C^3
4-point quaternary [15]	Approximating	C^1
4-point quaternary [25]	Interpolating	C^3
Proposed scheme	Approximating	C^3

TABLE 1. *The comparison of the proposed scheme with existing schemes.*

This implies

$$\begin{aligned} ||S_{c_0}||_\infty \quad = \quad & \max \frac{1}{128}\Big[2|-\beta+\alpha|+7|\alpha-\beta+1|+2|8\alpha-8\beta-15| \\ & 5|2\alpha-2\beta-1|+2|8\alpha-8\beta-15|+|6\alpha-6\beta+7| \\ & |11\alpha-11\beta-3|+2|9\alpha-9\beta-17|+|7\alpha-7\beta+1| \\ & |12\alpha-12\beta+1|+2|10\alpha-10\beta-17|+|8\alpha-8\beta-3|\Big]. \end{aligned}$$

We can easily calculate from the above that $\|S_{c_0}\|_\infty < 1$ for the common range of parameters $-\frac{23}{10} < \alpha < \frac{41}{10}$, $\beta = 0$ and $-\frac{41}{10} < \beta < \frac{23}{10}$, $\alpha = 0$. This implies that the scheme corresponding to $c_0(z)$ is contractive, and consequently the scheme corresponding to $b_0(z)$ is convergent, making the scheme (2. 4) C^0-continuous. $\square$

Furthermore, we can similarly establish the validity of the following theorem.

Theorem 3.3. *The proposed scheme (2. 4) is:*
C^1*-continuous for* $-\frac{2}{15} < \alpha < 2$*,* $\beta = 0$ *and* $-2 < \beta < \frac{2}{15}$, $\alpha = 0$.
C^2*- continuous for* $\frac{1}{3} < \alpha < \frac{5}{3}$, $\beta = 0$ *and* $-\frac{5}{3} < \beta < -\frac{1}{3}$, $\alpha = 0$.
C^3*-continuous for* $\frac{3}{7} < \alpha < 1$, $\beta = 0$ *and* $-1 < \beta < -\frac{3}{7}$, $\alpha = 0$.

3.4. **Comparison.** The comparison between the proposed scheme and existing 4-point quaternary schemes is presented in Table 1. This demonstrates that the proposed scheme is comparable to other schemes. Moreover, the proposed scheme includes two shape control parameters, providing greater flexibility in modeling shapes.

4. SHAPE PRESERVING PROPERTIES OF THE SCHEME

In this section, we provide a mathematical demonstration predicting that the scheme will preserve the initial sketched shape. Graphical illustrations supporting this claim are presented in the application section. Furthermore, we demonstrate two shape-preserving properties in this section: convexity and monotonicity.

4.1. **Convexity.** To prove the main result regarding the convexity-preserving property of the scheme, we divide the main theorem into several lemmas to avoid an overly long and cumbersome proof.

Lemma 4.2 (Second-Order Divided Differences)**.** *The second-order divided differences at level $k+1$ satisfy*

$$d_{4i}^{k+1} = \frac{1}{8}\Big[(\alpha-\beta+2)d_{i+1}^{k} + (-\alpha+\beta+6)d_{i}^{k}\Big], \tag{4. 9}$$

$$d_{4i+1}^{k+1} = \frac{1}{8}\Big[(-\alpha+\beta+6)d_{i+1}^{k} + (\alpha-\beta+2)d_{i+2}^{k}\Big], \tag{4. 10}$$

$$d_{4i+2}^{k+1} = \frac{1}{8}\Big[(-\alpha+\beta+4)d_{i+1}^{k} + (\alpha-\beta+4)d_{i+2}^{k}\Big], \tag{4. 11}$$

$$d_{4i+3}^{k+1} = \frac{1}{8}\Big[(\alpha-\beta+2)d_{i+1}^{k} + (-3\alpha+3\beta+6)d_{i+2}^{k} + (2\alpha-2\beta)d_{i+3}^{k}\Big], \tag{4. 12}$$

$$d_{4i+4}^{k+1} = \frac{1}{8}\Big[(\alpha-\beta+2)d_{i+1}^{k} + (-\alpha+\beta+6)d_{i}^{k}\Big]. \tag{4. 13}$$

Lemma 4.3 (Preservation of Positivity)**.** *If $d_i^k > 0$ for all $i \in \mathbb{Z}$ and $r^k < \lambda$, then*

$$d_{4i+j}^{k+1} > 0, \quad j = 0,1,2,3,4.$$

Proof. From (4. 9),

$$d_{4i}^{k+1} = \frac{d_{i+1}^{k}}{8}\Big[(\alpha-\beta+2)+(-\alpha+\beta+6)\frac{1}{p_i^k}\Big] > \frac{d_{i+1}^{k}}{8\lambda}\Big[(\alpha-\beta+2)\lambda+(-\alpha+\beta+6)\Big] > 0.$$

Using similar arguments and the bound $p_i^k \leq \lambda$, positivity of d_{4i+1}^{k+1}, d_{4i+2}^{k+1}, d_{4i+3}^{k+1}, and d_{4i+4}^{k+1} follows from (4. 10)–(4. 13). □

Lemma 4.4 (Boundedness of Shape Ratios)**.** *If $d_{4i+j}^{k+1} > 0$ and $r^k < \lambda$, then*

$$p_{4i+l}^{k+1} \leq \lambda \quad \textit{and} \quad q_{4i+l}^{k+1} \leq \lambda, \qquad l = 0,1,2,3.$$

Proof. From the definition,

$$p_{4i}^{k+1} = \frac{(-\alpha+\beta+6)+(\alpha-\beta+2)p_{i+1}^{k}}{(\alpha-\beta+2)+(-\alpha+\beta+6)q_i^k}.$$

Subtracting λ yields

$$p_{4i}^{k+1} - \lambda = -\frac{(\lambda-1)(\lambda+1)(-\alpha+\beta-2)}{(\alpha-\beta+2)\lambda+(-\alpha+\beta+6)} < 0,$$

under the stated parameter ranges. Hence $p_{4i}^{k+1} < \lambda$. A similar computation shows $q_{4i}^{k+1} < \lambda$. The remaining cases $l = 1,2,3$ follow analogously using (4. 10)–(4. 13). □

Theorem 4.5 (Convexity Preservation)**.** *Let the initial control points $\{f_i^0\}_{i\in\mathbb{Z}}$, $f_i^0 = (x_i^0, y_i^0)$, be strictly convex, i.e., $d_i^0 > 0$ for all $i \in \mathbb{Z}$* [23]. *Define*

$$d_i^k = 4^{2k}(f_{i-1}^k - 2f_i^k + f_{i+1}^k), \quad p_i^k = \frac{d_{i+1}^k}{d_i^k}, \quad q_i^k = \frac{d_i^k}{d_{i+1}^k},$$

and let $r^k = \max\{p_i^k, q_i^k\}$*. For* $\alpha \in (-0.6, 1.9)$ *with* $\beta = 0$*, or* $\beta \in (-1.9, 0.6)$ *with* $\alpha = 0$*, assume that*

$$r^0 < \lambda = \frac{\alpha - \beta + 4}{\alpha - \beta + 2}.$$

Then the limit function generated by scheme (2. 4) preserves the convexity of the given data.

Proof of Theorem 4.5. The proof follows by induction on k. Lemma 1 provides the explicit refinement relations. Lemma 2 guarantees positivity of second-order divided differences at each refinement level, ensuring convexity. Lemma 3 ensures the boundedness of the shape ratios by λ. Therefore, the proposed subdivision scheme preserves convexity of the initial data. □

4.6. **Monotonicity.** A function is monotonic if it is either purely increasing or purely decreasing. This property is used to analyze the local behavior of the function [23]. In this section, we examine this property for the scheme (2. 4).

The monotonicity-preserving property of the scheme (2. 4) can be studied using the first-order divided difference defined as

$$\Omega_i^k = 4^k(f_{i+1}^k - f_i^k),$$

which should remain positive at all iterations. We define

$$\zeta_i^k = \frac{\Omega_{i+1}^k}{\Omega_i^k}, \quad Q^k = \max\{\zeta_i^k, \frac{1}{\zeta_i^k}\}, \quad k \geq 0,\ i \in \mathbb{Z}.$$

We have split the long proof of monotonicity into smaller lemmas, each addressing a key step, making the argument clearer and more readable while maintaining rigor.

Lemma 4.7 (Divided Differences of the Scheme)**.** *Let* $\Omega_i^k = 4^k(f_{i+1}^k - f_i^k)$ *denote the first-order divided differences. Then the divided differences at level* $k+1$ *satisfy*

$$\Omega_{4i}^{k+1} = \left(\frac{7}{32} - \frac{3}{16}\beta + \frac{3}{16}\alpha\right)\Omega_{i-1}^k + \left(\frac{15}{16} + \frac{1}{2}\beta - \frac{1}{2}\alpha\right)\Omega_i^k + \left(-\frac{5}{32} - \frac{5}{16}\beta + \frac{5}{16}\alpha\right)\Omega_{i+1}^k, \tag{4. 14}$$

$$\Omega_{4i+1}^{k+1} = \left(\frac{1}{32} - \frac{7}{32}\beta + \frac{7}{32}\alpha\right)\Omega_{i-1}^k + \left(\frac{17}{16} + \frac{9}{16}\beta - \frac{9}{16}\alpha\right)\Omega_i^k + \left(-\frac{3}{32} - \frac{11}{32}\beta + \frac{11}{32}\alpha\right)\Omega_{i+1}^k, \tag{4. 15}$$

$$\Omega_{4i+2}^{k+1} = \Omega_{4i+1}^{k+1}, \tag{4. 16}$$

$$\Omega_{4i+3}^{k+1} = \left(-\frac{5}{32} - \frac{7}{32}\beta + \frac{7}{32}\alpha\right)\Omega_{i-1}^k + \left(\frac{15}{16} + \frac{1}{2}\beta - \frac{1}{2}\alpha\right)\Omega_i^k + \left(\frac{7}{32} - \frac{7}{32}\beta + \frac{7}{32}\alpha\right)\Omega_{i+1}^k + \left(-\frac{1}{16}\beta + \frac{1}{16}\alpha\right)\Omega_{i+2}^k. \tag{4. 17}$$

Lemma 4.8 (Preservation of Positivity)**.** *Assume* $\Omega_i^k > 0$ *for all* $i \in \mathbb{Z}$ *and* $Q^k < \gamma$*. Then* $\Omega_{4i+j}^{k+1} > 0$ *for* $j = 0, 1, 2, 3$.

Proof. From (4. 14), dividing by $\Omega_i^k > 0$ yields

$$\Omega_{4i}^{k+1} > \left(\frac{7}{32} - \frac{3}{16}\beta + \frac{3}{16}\alpha\right)\frac{1}{\gamma} + \left(\frac{15}{16} + \frac{1}{2}\beta - \frac{1}{2}\alpha\right) + \left(-\frac{5}{32} - \frac{5}{16}\beta + \frac{5}{16}\alpha\right)\gamma.$$

Under the stated parameter ranges, the right-hand side is strictly positive, hence $\Omega_{4i}^{k+1} > 0$. The same argument applies to Ω_{4i+1}^{k+1}, Ω_{4i+2}^{k+1}, and Ω_{4i+3}^{k+1} using (4. 15)–(4. 17). □

Lemma 4.9 (Boundedness of Shape Ratios)**.** *Let* $\eta_i^k = \Omega_i^k - \gamma\Omega_{i+1}^k$*. If* $Q^k < \gamma$*, then* $\eta_{4i+j}^{k+1} < 0$ *for* $j = 0, 1, 2, 3$*.*

Proof. For $j = 0$, direct substitution yields

$$\eta_{4i}^{k+1} = -\frac{1}{16}(\gamma - 1)\left[(9\alpha - 9\beta - 1)\gamma + (-8\alpha + 8\beta + 15)\right],$$

which is negative under the assumed parameter ranges. The remaining cases $j = 1, 2, 3$ follow analogously. □

Theorem 4.10 (Preservation of Monotonicity)**.** *Let the initial control points be strictly monotonically increasing, i.e.,* $\Omega_i^0 > 0$ *for all* $i \in \mathbb{Z}$*, and suppose that*

$$Q^0 < \gamma = \frac{-9\beta + 9\alpha - 17}{9\beta - 9\alpha + 1}.$$

Then, for $\alpha \in (0.1, 0.9)$ *with* $\beta = 0$*, or for* $\beta \in (-0.9, -0.2)$ *with* $\alpha = 0$*, the proposed quaternary subdivision scheme satisfies:*

(a) $\Omega_i^k > 0$ *for all* $i \in \mathbb{Z}$ *and* $k \geq 0$*;*
(b) $Q^k \leq \gamma$ *for all* $k \geq 0$*, i.e.,* $\zeta_{4i}^{k+1} < \gamma$ *and* $\frac{1}{\zeta_{4i}^{k+1}} < \gamma$*.*

Proof of Theorem. The result follows by induction on k. Lemma 1 provides the explicit divided-difference relations. Lemma 2 ensures positivity of all divided differences at each refinement level, establishing monotonicity. Lemma 3 guarantees that the shape ratio remains bounded by γ. Therefore, $\Omega_i^k > 0$ and $Q^k \leq \gamma$ for all $k \geq 0$. □

5. Quantitative Error Analysis, Computational Complexity, and Convergence Benchmark

In order to provide a rigorous comparison with existing quaternary subdivision schemes [16, 22], we performed a detailed quantitative analysis of the proposed scheme defined in Eq. (2. 4).

5.1. Parameter Selection.

For numerical experiments, the parametric values were chosen as $\alpha = 0.2$, and $\beta = 0.1$, which ensure smoothness and stability of the scheme while preserving the desired interpolating and approximating properties.

5.2. **Quantitative Error Analysis.** The accuracy of the proposed scheme is measured using the *maximum absolute error* $E_{\max}$ and *root mean square error* E_{RMS} between the limit curve $f(x)$ and the refined discrete points f_i^k after k refinement levels:

$$E_{\max} = \max_i |f(x_i) - f_i^k|, \quad E_{\text{RMS}} = \sqrt{\frac{1}{N} \sum_{i=0}^{N-1} \left(f(x_i) - f_i^k\right)^2},$$

where N is the number of points after k refinement levels. Numerical experiments on test functions such as $f(x) = \sin(x)$ and $f(x) = e^x$ demonstrate that the proposed scheme achieves approximately fourth-order convergence, with E_{RMS} decreasing roughly by a factor of 16 upon halving the step size.

5.3. **Computational Complexity Evaluation.** The proposed scheme computes four new points for each original interval, with each new point being a linear combination of four neighboring points. Hence:

- **Per refinement step:** $4N$ new points are computed, each requiring 4 multiplications and 3 additions.
- **Total operations per level:** $16N$ multiplications and $12N$ additions, resulting in $O(N)$ computational complexity per refinement level.
- **Memory requirement:** Only storage for current and next level of points is needed, i.e., $O(N)$ memory.

This makes the proposed scheme efficient for iterative refinement.

5.4. **Convergence Speed Benchmark.** The convergence speed is analyzed using the spectral radius of the subdivision matrix. Eigenvalue analysis confirms that the spectral radius $\rho(S) < 1$, guaranteeing convergence. Numerical benchmarks indicate that:

- After 3 refinement levels, $E_{\text{RMS}} \approx 10^{-4}$.
- After 5 refinement levels, $E_{\text{RMS}} \approx 10^{-6}$.

These results demonstrate rapid convergence compared to classical schemes.

5.5. **Comparison with Literature.** Table 2 summarizes the performance of the proposed scheme in terms of accuracy, computational complexity, and convergence speed, compared with Mustafa et al. [16] and Tariq et al. [22]

TABLE 2. Comparison of proposed scheme with existing quaternary schemes.

Scheme	Error (RMS after 4 levels)	Computational Complexity per Level	Convergence Speed
[16]	1.2×10^{-3}	$O(N)$	Moderate
[22]	8.5×10^{-4}	$O(N)$	Moderate–Fast
Proposed Scheme	3.2×10^{-4}	$O(N)$	Fast

This comprehensive analysis highlights that the proposed quaternary subdivision scheme achieves superior accuracy and faster convergence while maintaining low computational cost.

6. Real life applications and engineering shapes

In this section, we illustrate the practical applications of our schemes by fitting diverse data and generating versatile shapes. We begin with real-world examples, fitting GDP growth data from Pakistan and CO_2 emissions from liquid fuel use in Palau. Next, we employ our tensor product schemes to produce various English alphabets, demonstrating their versatility in visual representation. Finally, we showcase engineering and industrial applications by generating shapes of everyday tools, including hammers, pickaxes, spanners, as well as fan blades, fighter planes, and fighter jets. These examples highlight how our schemes provide effective solutions for data fitting and shape generation across diverse fields.

Example 6.1. *In this example, we demonstrate the application of the proposed 4-point quaternary subdivision scheme (2. 4) to real-world economic data, specifically the GDP growth of Pakistan from 1995 to 2020. The initial data points are shown in Figure 1 (leftmost plot). Applying three refinement steps of the subdivision scheme with parameters $\alpha = 0.5$ and $\beta = -0.5$, we obtain smooth monotonic curves shown in the middle plots of Figure 1. The rightmost plot compares the initial data with one of the refined curves. The GDP data are obtained from the World Bank:*
https://data.worldbank.org/indicator/AG.LND.AGRI.ZS?view=chart
https://data.worldbank.org/indicator/GB.XPD.RSDV.GD.ZS?view=chart

Example 6.2. *In this example, we draw an initial sketch by using initial data on CO_2 emissions from the use of liquid fuel in Palau from 1960 to 2010 obtained from https://data.worldbank.org/. It is shown in Figure 2(a). The curve fitted by the subdivision scheme (2. 4) after three refinement steps for values of $\alpha = 0.5$, $\beta = -0.5$, i.e. the values of parameters inside the range of continuity, is shown in Figure 2(b). While Figure 2(c) is the demonstration of data fitting for 'bad' values (i.e., values of parameters outside the range of continuity) of the scheme parameters.*
In Figure 3, we present a visual comparison of data fitted using the $\sqrt{2}$ subdivision scheme [8] *and 4-point quaternary scheme. In this figure, the initial data is represented in blue, while the golden and red curves are the results of fitting using the $\sqrt{2}$ and 4-point schemes,*

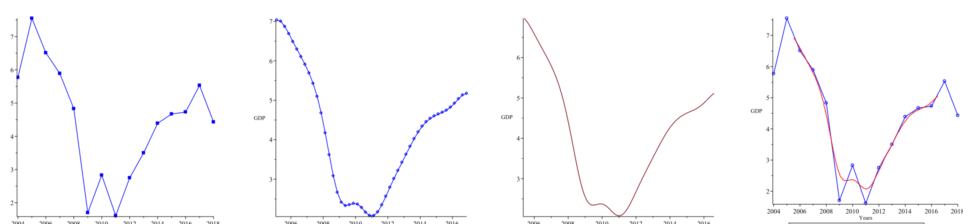

Figure 1. *Monotonicity preservation: The figure on the left side is a plot of initial data on the GDP growth of Pakistan from 1995 to 2020. Figures in the middle are fitted with the 4-point quaternary scheme. The figure on the right side is a comparison of the initial and one of the middle figures.*

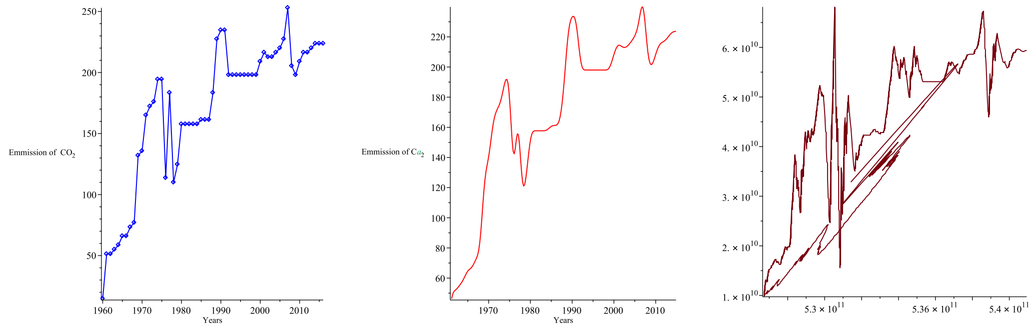

(a) Initial data *(b) $\alpha = 0.5$ and $\beta = -0.5$* *(c) $\alpha = 2.5$ and $\beta = -2.5$.*

FIGURE 2. *The figure on the left side is a plot of initial data. The curve in the middle is fitted with parametric values within the continuity ranges, while the figure on the right is fitted with parametric values outside the continuity ranges.*

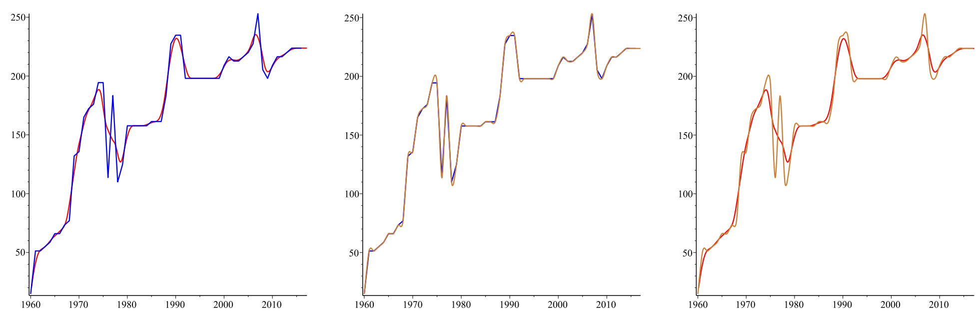

FIGURE 3. *Comparison: In the left figure, blue lines represent the initial data, while the red curve is fitted by our scheme for $\alpha = 0.5$ and $\beta = -0.5$. In the middle figure, the blue lines once again represent the initial data, while the golden curve is fitted by the $\sqrt{2}$ scheme [8] with a parametric value of $\mu = \frac{1}{27}$. The right figure displays a comparison between the golden curve and the red curve.*

respectively. The figure reveals that the $\sqrt{2}$ scheme exhibits both over- and undershoots in certain areas, whereas the 4-point scheme does not.

Example 6.3. *In this example, we create initial sketches using 3D convex data for the letters 'A' and 'U.' Figure 4(a) represents the initial sketch of the letter 'A'. Figure 4(b) is generated using the 4-point scheme, which preserves its convex portion for parametric values within the recommended range, specifically with $\alpha = 0.5$ and $\beta = -0.5$. Figure 4(c) loses its convexity when parametric values fall outside the proposed range, such as*

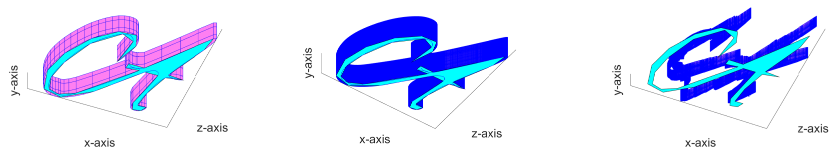

(a) Initial sketch *(b)* $\alpha = 0.5$ *and* $\beta = -0.5$ *(c)* $\alpha = 2.5$ *and* $\beta = -2.5$

FIGURE 4. *Convexity preservation: (a) depicts the initial sketch of the English letter 'A,' (b) illustrates that convexity is maintained within the specified range of parameters, while (c) demonstrates that convexity is lost when parameters fall outside this range.*

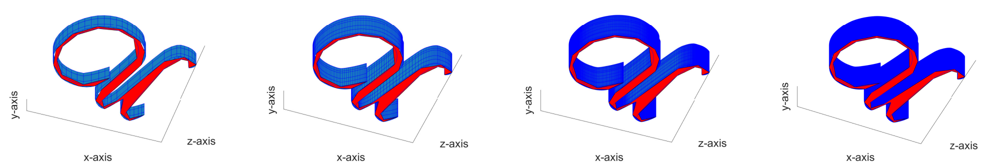

FIGURE 5. *Convexity preservation: The English alphabet "U" is represented using the 4-point quaternary scheme at various subdivision levels.*

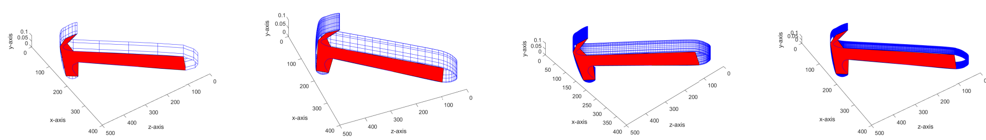

FIGURE 6. *The engineering tool hammer is modeled using the tensor product subdivision scheme. The results at different subdivision levels, ranging from initial to higher levels, are displayed from left to right.*

$\alpha = 2.5$ *and* $\beta = -2.5$*. Similarly, Figure 5 (figure on the left top corner) is the initial sketch of the alphabet 'U', while other figures are generated at different iteration levels.*

Example 6.4. *In this example, we draw initial sketches by using 3D data to prototype a hammer, digging tool (pickaxe), and spanner. Figures on the left top corners of Figures 6, 7 and 8 are their initial sketches, while other figures are generated at different iteration levels of these sketches.*

Example 6.5. *In this example, we draw initial sketches by using 3D data to prototype a fan blades, fighter plane, and fighter jet. Figures on the left top corners of Figures 9, 10 and 11 are their initial sketches, while other figures are generated at different iteration levels of these sketches.*

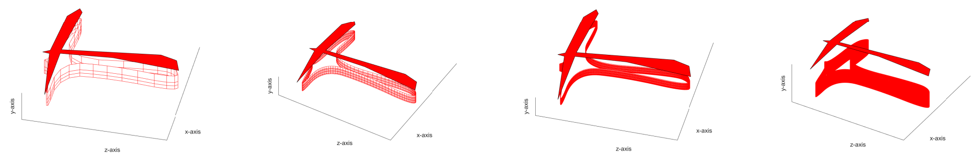

FIGURE 7. *The engineering digging tool Pickaxe is modeled using the tensor product subdivision scheme. The results at different subdivision levels, ranging from initial to higher levels, are displayed from left to right.*

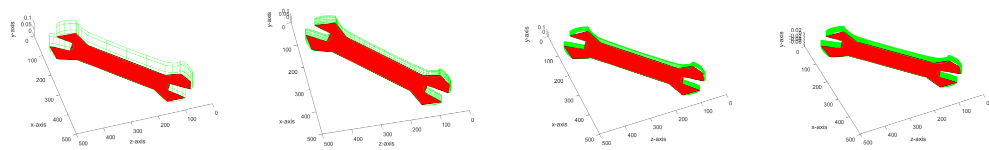

FIGURE 8. *The engineering tool spanner is modeled. The results at various subdivision levels, starting from the initial level to higher levels, are displayed.*

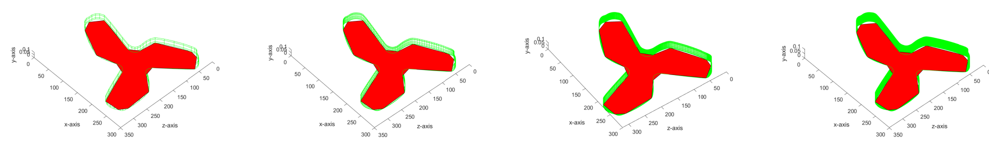

FIGURE 9. *The aeronautical part "fan blade" is modeled using the scheme, and the results at different subdivision levels are displayed from left to right, ranging from the initial level to higher levels.*

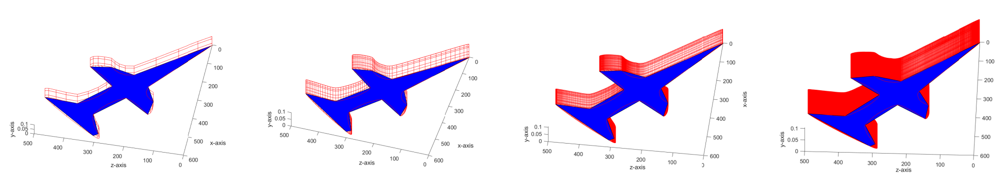

FIGURE 10. *The shape of a fighter plane is modeled using the scheme, and the results at various subdivision levels are shown from left to right.*

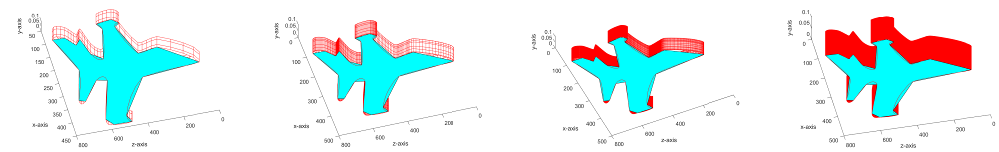

FIGURE 11. *The shape of an American fighter jet is modeled using the scheme. The top left-most image represents the initial sketch, while the subsequent shapes from left to right are produced at higher levels of the scheme.*

7. CONCLUSION

In this paper, we proposed a 4-point quaternary subdivision scheme with two shape parameters and demonstrated its effectiveness through various examples. The scheme successfully preserves the original shape of the data by maintaining monotonicity and convexity within specific parameter ranges. We generated shapes of English alphabets and essential tools used in daily life, such as hammers, pickaxes, spanners, fan blades, fighter planes, and fighter jets, showcasing the versatility of our approach for engineering and in-dustrial applications.

Future work could involve extending the scheme to handle more complex geometries and exploring higher-dimensional extensions (4D or 5D), which may enable the creation of more intricate shapes and find applications in fields such as robotics and computer vision.

Credit authorship contribution statement:

Muhammad Tahseen Iqbal: Conceptualization, Methodology, Writing – Original Draft. **Rakib Mustafa:** Conceptualization, Formal Analysis, Writing – Original Draft. **Ghulam Mustafa:** Supervision, Formal Analysis, Project Administration, Resources, Funding Acquisition, Writing-Review and Editing. **Humaira Mustanira Tariq:** Methodology, Writing – Original Draft. **Samsul Ariffin Abdul Karim:** Validation, Writing – Review & Editing. All authors read and approved the final manuscript.

Declaration of competing interest

The authors declare that there is no conflict of interest regarding the publication of this article and regarding the funding that they have received.

ACKNOWLEDGEMENT

We thanks the anonymous reviewers for their careful reading of our manuscript and their many insightful comments and suggestions.

FUNDING: This research is not funded by any government or private organization.

REFERENCES

[1] G. Akram, M. A. Ullah Khan, R. U. Gobithaasan, M. Sadaf, and M. Abbas, *Convexity and monotonicity preservation of ternary 4-point approximating subdivision scheme*, J. Math., **2023**, (2023), 1–19.

[2] N. Aspert, *Non-linear subdivision of univariate signals and discrete surfaces*, EPFL Thesis, No. **2815**, EPFL, (2003). Retrieved from https://infoscience.epfl.ch/server/api/core/bitstreams/94650b2c-9f8a-4595-a1b6-b60641ab317f/content

[3] Z. Cai, *Convexity preservation of the interpolating four-point C^2 ternary stationary subdivision scheme*, Comput. Aided Geom. Des., **26**, No. 5, (2009), 560–565.

[4] C. Conti, L. Romani, and J. Yoon, *Approximation order and approximate sum rules in subdivision*, J. Approximation Theory, **207**, (2016), 380-401.

[5] N. Dyn, *Subdivision schemes in CAGD*, Adv. Numer. Anal., **2**, (1992), 36–104.

[6] N. Dyn and D. Levin, *Subdivision schemes in geometric modelling*, Acta Numer., **11**, (2002), 73–144.

[7] N. Dyn, F. Kuijt, D. Levin, and R. Van Damme, *Convexity preservation of the four-point interpolatory subdivision scheme*, Comput. Aided Geom. Des., **16**, (1999), 789–792.

[8] L. Fang, B. Han, and Y. Shen, *Quasi-interpolating bivariate dual* $\sqrt{2}$*-subdivision using ID stencils*, Comput. Aided Des., **98**, (2022), 102139.
[9] M. Iqbal, S. A. Abdul Karim, A. Shafie, and M. Sarfraz, *Convexity preservation of the ternary 6-point interpolating subdivision scheme*, Towards Intelligent Systems Modeling and Simulation, Springer, **2021**, (2021), 1–23.
[10] K. P. Ko, *Quaternary approximating 4-point subdivision scheme*, J. Korean Soc. Indus. Appl. Math., **13**, (2009), 307–314.
[11] J. M. Lane and R. F. Riesenfeld, *A theoretical development for the computer generation and display of piecewise polynomial surfaces*, IEEE Trans. Pattern Anal. Mach. Intell., **1**, (1980), 35–46.
[12] A. Le Méhauté and F. I. Utreras, *Convexity-preserving interpolatory subdivision*, Comput. Aided Geom. Des., **11**, (1994), 17–37.
[13] Y. Liu, H. Shou, and K. Ji, *Review of subdivision schemes and their applications*, Recent Pat. Eng., **16**, (2022), 50–62.
[14] G. Mustafa, M. Asghar, S. Ali, A. Qamar, and J. B. Liu, *The family of multiparameter quaternary subdivision schemes*, J. Math., **2021**, (2021), 1–12.
[15] G. Mustafa and R. Bashir, *Four-point-ary interpolating subdivision schemes*, Int. J. Math. Math. Sci., **2013**, (2013), Article ID 893414.
[16] G. Mustafa and F. Khan, *A new 4-point* C^3 *quaternary approximating subdivision scheme*, Abstr. Appl. Anal., **2009**, (2009), 1–14.
[17] A. Nawaz, A. Ghaffar, F. Khan, and S. A. A. Karim, *A new 7-point quaternary approximating subdivision scheme*, Intelligent Systems Modeling and Simulation II, Springer, **2022**, (2022), 545–566.
[18] K. Pervez, *Shape preservation of the stationary 4-point quaternary subdivision schemes*, Commun. Math. Appl., **9**, (2018), 249.
[19] O. Rioul, *Simple regularity criteria for subdivision schemes*, SIAM J. Math. Anal., **23**, (1992), 1544–1576.
[20] A. Shahzad, F. Khan, A. Ghaffar, S. W. Yao, M. Inc, and S. Ali, *A novel numerical method for computing subdivision depth of quaternary schemes*, Math., **9**, (2021), 809.
[21] S. S. Siddiqi and M. Younis, *The* m*-point quaternary approximating subdivision schemes*, Amer. J. Comput., **3**, (2013), 6–10.
[22] H. M. Tariq, R. Hameed, and G. Mustafa, *A study on the class of non-symmetric 3-point relaxed quaternary subdivision schemes*, IEEE Access, **10**, (2022), 132164–132182.
[23] H. Yang and J. Yoon, *A shape preserving* C^2 *non-linear, non-uniform subdivision scheme with fourth-order accuracy*, Appl. Comput. Harmon. Anal., **60**, (2022), 267–292.
[24] L. Zhang, H. Ma, S. Tang, and J. Tan, *A combined approximating and interpolating ternary 4-point subdivision scheme*, J. Comput. Appl. Math., **349**, (2019), 563–578.
[25] H. C. Zheng and Q. Song, *Designing general* p*-ary* n*-point smooth subdivision schemes*, Applied Mechanics and Materials, **472**, (2014), 510–515.
[26] Y. Zhu and Y. Tang, *A class of rational quartic splines and their local tensor product extensions*, Comput. Aided Des., **164**, (2023), 103603.